

Improved Top Quark Mass Measurement in the Lepton + Jets Topology at CDF II

A. Abulencia,²³ D. Acosta,¹⁷ J. Adelman,¹³ T. Affolder,¹⁰ T. Akimoto,⁵³ M.G. Albrow,¹⁶
D. Ambrose,¹⁶ S. Amerio,⁴² D. Amidei,³³ A. Anastassov,⁵⁰ K. Anikeev,¹⁶ A. Annovi,⁴⁴
J. Antos,¹ M. Aoki,⁵³ G. Apollinari,¹⁶ J.-F. Arguin,³² T. Arisawa,⁵⁵ A. Artikov,¹⁴
W. Ashmanskas,¹⁶ A. Attal,⁸ F. Azfar,⁴¹ P. Azzi-Bacchetta,⁴² P. Azzurri,⁴⁴ N. Bacchetta,⁴²
H. Bachacou,²⁸ W. Badgett,¹⁶ A. Barbaro-Galtieri,²⁸ V.E. Barnes,⁴⁶ B.A. Barnett,²⁴
S. Baroiant,⁷ V. Bartsch,³⁰ G. Bauer,³¹ F. Bedeschi,⁴⁴ S. Behari,²⁴ S. Belforte,⁵²
G. Bellettini,⁴⁴ J. Bellinger,⁵⁷ A. Belloni,³¹ E. Ben-Haim,¹⁶ D. Benjamin,¹⁵ A. Beretvas,¹⁶
J. Beringer,²⁸ T. Berry,²⁹ A. Bhatti,⁴⁸ M. Binkley,¹⁶ D. Bisello,⁴² M. Bishai,¹⁶ R. E. Blair,²
C. Blocker,⁶ K. Bloom,³³ B. Blumenfeld,²⁴ A. Bocci,⁴⁸ A. Bodek,⁴⁷ V. Boisvert,⁴⁷
G. Bolla,⁴⁶ A. Bolshov,³¹ D. Bortoletto,⁴⁶ J. Boudreau,⁴⁵ S. Bourov,¹⁶ A. Boveia,¹⁰
B. Brau,¹⁰ C. Bromberg,³⁴ E. Brubaker,¹³ J. Budagov,¹⁴ H.S. Budd,⁴⁷ S. Budd,²³
K. Burkett,¹⁶ G. Busetto,⁴² P. Bussey,²⁰ K. L. Byrum,² S. Cabrera,¹⁵ M. Campanelli,¹⁹
M. Campbell,³³ F. Canelli,⁸ A. Canepa,⁴⁶ D. Carlsmith,⁵⁷ R. Carosi,⁴⁴ S. Carron,¹⁵
M. Casarsa,⁵² A. Castro,⁵ P. Catastini,⁴⁴ D. Cauz,⁵² M. Cavalli-Sforza,³ A. Cerri,²⁸
L. Cerrito,⁴¹ S.H. Chang,²⁷ J. Chapman,³³ Y.C. Chen,¹ M. Chertok,⁷ G. Chiarelli,⁴⁴
G. Chlachidze,¹⁴ F. Chlebana,¹⁶ I. Cho,²⁷ K. Cho,²⁷ D. Chokheli,¹⁴ J.P. Chou,²¹
P.H. Chu,²³ S.H. Chuang,⁵⁷ K. Chung,¹² W.H. Chung,⁵⁷ Y.S. Chung,⁴⁷ M. Ciljak,⁴⁴
C.I. Ciobanu,²³ M.A. Ciocci,⁴⁴ A. Clark,¹⁹ D. Clark,⁶ M. Coca,¹⁵ A. Connolly,²⁸
M.E. Convery,⁴⁸ J. Conway,⁷ B. Cooper,³⁰ K. Copic,³³ M. Cordelli,¹⁸ G. Cortiana,⁴²
A. Cruz,¹⁷ J. Cuevas,¹¹ R. Culbertson,¹⁶ D. Cyr,⁵⁷ S. DaRonco,⁴² S. D'Auria,²⁰
M. D'onofrio,¹⁹ D. Dagenhart,⁶ P. de Barbaro,⁴⁷ S. De Cecco,⁴⁹ A. Deisher,²⁸
G. De Lentdecker,⁴⁷ M. Dell'Orso,⁴⁴ S. Demers,⁴⁷ L. Demortier,⁴⁸ J. Deng,¹⁵ M. Deninno,⁵
D. De Pedis,⁴⁹ P.F. Derwent,¹⁶ C. Dionisi,⁴⁹ J. Dittmann,⁴ P. DiTuro,⁵⁰ C. Dörr,²⁵
A. Dominguez,²⁸ S. Donati,⁴⁴ M. Donega,¹⁹ P. Dong,⁸ J. Donini,⁴² T. Dorigo,⁴² S. Dube,⁵⁰
K. Ebina,⁵⁵ J. Efron,³⁸ J. Ehlers,¹⁹ R. Erbacher,⁷ D. Errede,²³ S. Errede,²³ R. Eusebi,⁴⁷
H.C. Fang,²⁸ S. Farrington,²⁹ I. Fedorko,⁴⁴ W.T. Fedorko,¹³ R.G. Feild,⁵⁸ M. Feindt,²⁵
J.P. Fernandez,⁴⁶ R. Field,¹⁷ G. Flanagan,³⁴ L.R. Flores-Castillo,⁴⁵ A. Foland,²¹
S. Forrester,⁷ G.W. Foster,¹⁶ M. Franklin,²¹ J.C. Freeman,²⁸ Y. Fujii,²⁶ I. Furic,¹³

A. Gajjar,²⁹ M. Gallinaro,⁴⁸ J. Galyardt,¹² J.E. Garcia,⁴⁴ M. Garcia Sciveres,²⁸
 A.F. Garfinkel,⁴⁶ C. Gay,⁵⁸ H. Gerberich,²³ E. Gerchtein,¹² D. Gerdes,³³ S. Giagu,⁴⁹
 P. Giannetti,⁴⁴ A. Gibson,²⁸ K. Gibson,¹² C. Ginsburg,¹⁶ K. Giolo,⁴⁶ M. Giordani,⁵²
 M. Giunta,⁴⁴ G. Giurciu,¹² V. Glagolev,¹⁴ D. Glenzinski,¹⁶ M. Gold,³⁶ N. Goldschmidt,³³
 J. Goldstein,⁴¹ G. Gomez,¹¹ G. Gomez-Ceballos,¹¹ M. Goncharov,⁵¹ O. González,⁴⁶
 I. Gorelov,³⁶ A.T. Goshaw,¹⁵ Y. Gotra,⁴⁵ K. Goulianos,⁴⁸ A. Gresele,⁴² M. Griffiths,²⁹
 S. Grinstein,²¹ C. Grosso-Pilcher,¹³ U. Grundler,²³ J. Guimaraes da Costa,²¹ C. Haber,²⁸
 S.R. Hahn,¹⁶ K. Hahn,⁴³ E. Halkiadakis,⁴⁷ A. Hamilton,³² B.-Y. Han,⁴⁷ R. Handler,⁵⁷
 F. Happacher,¹⁸ K. Hara,⁵³ M. Hare,⁵⁴ S. Harper,⁴¹ R.F. Harr,⁵⁶ R.M. Harris,¹⁶
 K. Hatakeyama,⁴⁸ J. Hauser,⁸ C. Hays,¹⁵ H. Hayward,²⁹ A. Heijboer,⁴³ B. Heinemann,²⁹
 J. Heinrich,⁴³ M. Hennecke,²⁵ M. Herndon,⁵⁷ J. Heuser,²⁵ D. Hidas,¹⁵ C.S. Hill,¹⁰
 D. Hirschbuehl,²⁵ A. Hocker,¹⁶ A. Holloway,²¹ S. Hou,¹ M. Houlden,²⁹ S.-C. Hsu,⁹
 B.T. Huffman,⁴¹ R.E. Hughes,³⁸ J. Huston,³⁴ K. Ikado,⁵⁵ J. Incandela,¹⁰ G. Introzzi,⁴⁴
 M. Iori,⁴⁹ Y. Ishizawa,⁵³ A. Ivanov,⁷ B. Iyutin,³¹ E. James,¹⁶ D. Jang,⁵⁰ B. Jayatilaka,³³
 D. Jeans,⁴⁹ H. Jensen,¹⁶ E.J. Jeon,²⁷ M. Jones,⁴⁶ K.K. Joo,²⁷ S.Y. Jun,¹² T.R. Junk,²³
 T. Kamon,⁵¹ J. Kang,³³ M. Karagoz-Unel,³⁷ P.E. Karchin,⁵⁶ Y. Kato,⁴⁰ Y. Kemp,²⁵
 R. Kephart,¹⁶ U. Kerzel,²⁵ V. Khotilovich,⁵¹ B. Kilminster,³⁸ D.H. Kim,²⁷ H.S. Kim,²⁷
 J.E. Kim,²⁷ M.J. Kim,¹² M.S. Kim,²⁷ S.B. Kim,²⁷ S.H. Kim,⁵³ Y.K. Kim,¹³ M. Kirby,¹⁵
 L. Kirsch,⁶ S. Klimenko,¹⁷ M. Klute,³¹ B. Knuteson,³¹ B.R. Ko,¹⁵ H. Kobayashi,⁵³
 K. Kondo,⁵⁵ D.J. Kong,²⁷ J. Konigsberg,¹⁷ K. Kordas,¹⁸ A. Korytov,¹⁷ A.V. Kotwal,¹⁵
 A. Kovalev,⁴³ J. Kraus,²³ I. Kravchenko,³¹ M. Kreps,²⁵ A. Kreymer,¹⁶ J. Kroll,⁴³
 N. Krumnack,⁴ M. Kruse,¹⁵ V. Krutelyov,⁵¹ S. E. Kuhlmann,² Y. Kusakabe,⁵⁵ S. Kwang,¹³
 A.T. Laasanen,⁴⁶ S. Lai,³² S. Lami,⁴⁴ S. Lammel,¹⁶ M. Lancaster,³⁰ R.L. Lander,⁷
 K. Lannon,³⁸ A. Lath,⁵⁰ G. Latino,⁴⁴ I. Lazzizzera,⁴² C. Lecci,²⁵ T. LeCompte,²
 J. Lee,⁴⁷ J. Lee,²⁷ S.W. Lee,⁵¹ R. Lefèvre,³ N. Leonardo,³¹ S. Leone,⁴⁴ S. Levy,¹³
 J.D. Lewis,¹⁶ K. Li,⁵⁸ C. Lin,⁵⁸ C.S. Lin,¹⁶ M. Lindgren,¹⁶ E. Lipeles,⁹ T.M. Liss,²³
 A. Lister,¹⁹ D.O. Litvintsev,¹⁶ T. Liu,¹⁶ Y. Liu,¹⁹ N.S. Lockyer,⁴³ A. Loginov,³⁵
 M. Loreti,⁴² P. Loverre,⁴⁹ R.-S. Lu,¹ D. Lucchesi,⁴² P. Lujan,²⁸ P. Lukens,¹⁶ G. Lungu,¹⁷
 L. Lyons,⁴¹ J. Lys,²⁸ R. Lysak,¹ E. Lytken,⁴⁶ P. Mack,²⁵ D. MacQueen,³² R. Madrak,¹⁶
 K. Maeshima,¹⁶ P. Maksimovic,²⁴ G. Manca,²⁹ F. Margaroli,⁵ R. Marginean,¹⁶

C. Marino,²³ A. Martin,⁵⁸ M. Martin,²⁴ V. Martin,³⁷ M. Martínez,³ T. Maruyama,⁵³
 H. Matsunaga,⁵³ M.E. Mattson,⁵⁶ R. Mazini,³² P. Mazzanti,⁵ K.S. McFarland,⁴⁷
 D. McGivern,³⁰ P. McIntyre,⁵¹ P. McNamara,⁵⁰ R. McNulty,²⁹ A. Mehta,²⁹ S. Menzemer,³¹
 A. Menzione,⁴⁴ P. Merkel,⁴⁶ C. Mesropian,⁴⁸ A. Messina,⁴⁹ M. von der Mey,⁸ T. Miao,¹⁶
 N. Miladinovic,⁶ J. Miles,³¹ R. Miller,³⁴ J.S. Miller,³³ C. Mills,¹⁰ M. Milnik,²⁵ R. Miquel,²⁸
 S. Miscetti,¹⁸ G. Mitselmakher,¹⁷ A. Miyamoto,²⁶ N. Moggi,⁵ B. Mohr,⁸ R. Moore,¹⁶
 M. Morello,⁴⁴ P. Movilla Fernandez,²⁸ J. Mülmenstädt,²⁸ A. Mukherjee,¹⁶ M. Mulhearn,³¹
 Th. Muller,²⁵ R. Mumford,²⁴ P. Murat,¹⁶ J. Nachtman,¹⁶ S. Nahn,⁵⁸ I. Nakano,³⁹
 A. Napier,⁵⁴ D. Naumov,³⁶ V. Necula,¹⁷ C. Neu,⁴³ M.S. Neubauer,⁹ J. Nielsen,²⁸
 T. Nigmanov,⁴⁵ L. Nodulman,² O. Norniella,³ T. Ogawa,⁵⁵ S.H. Oh,¹⁵ Y.D. Oh,²⁷
 T. Okusawa,⁴⁰ R. Oldeman,²⁹ R. Orava,²² K. Osterberg,²² C. Pagliarone,⁴⁴ E. Palencia,¹¹
 R. Paoletti,⁴⁴ V. Papadimitriou,¹⁶ A. Papikononou,²⁵ A.A. Paramonov,¹³ B. Parks,³⁸
 S. Pashapour,³² J. Patrick,¹⁶ G. Pauletta,⁵² M. Paulini,¹² C. Paus,³¹ D.E. Pellett,⁷
 A. Penzo,⁵² T.J. Phillips,¹⁵ G. Piacentino,⁴⁴ J. Piedra,¹¹ K. Pitts,²³ C. Plager,⁸
 L. Pondrom,⁵⁷ G. Pope,⁴⁵ X. Portell,³ O. Poukhov,¹⁴ N. Pounder,⁴¹ F. Prakoshyn,¹⁴
 A. Pronko,¹⁶ J. Proudfoot,² F. Ptohos,¹⁸ G. Punzi,⁴⁴ J. Pursley,²⁴ J. Rademacker,⁴¹
 A. Rahaman,⁴⁵ A. Rakitin,³¹ S. Rappoccio,²¹ F. Ratnikov,⁵⁰ B. Reisert,¹⁶ V. Rekovic,³⁶
 N. van Remortel,²² P. Renton,⁴¹ M. Rescigno,⁴⁹ S. Richter,²⁵ F. Rimondi,⁵ K. Rinnert,²⁵
 L. Ristori,⁴⁴ W.J. Robertson,¹⁵ A. Robson,²⁰ T. Rodrigo,¹¹ E. Rogers,²³ S. Rolli,⁵⁴
 R. Roser,¹⁶ M. Rossi,⁵² R. Rossin,¹⁷ C. Rott,⁴⁶ A. Ruiz,¹¹ J. Russ,¹² V. Rusu,¹³
 D. Ryan,⁵⁴ H. Saarikko,²² S. Sabik,³² A. Safonov,⁷ W.K. Sakumoto,⁴⁷ G. Salamanna,⁴⁹
 O. Salto,³ D. Saltzberg,⁸ C. Sanchez,³ L. Santi,⁵² S. Sarkar,⁴⁹ K. Sato,⁵³ P. Savard,³²
 A. Savoy-Navarro,¹⁶ T. Scheidle,²⁵ P. Schlabach,¹⁶ E.E. Schmidt,¹⁶ M.P. Schmidt,⁵⁸
 M. Schmitt,³⁷ T. Schwarz,³³ L. Scodellaro,¹¹ A.L. Scott,¹⁰ A. Scribano,⁴⁴ F. Scuri,⁴⁴
 A. Sedov,⁴⁶ S. Seidel,³⁶ Y. Seiya,⁴⁰ A. Semenov,¹⁴ F. Semeria,⁵ L. Sexton-Kennedy,¹⁶
 I. Sfiligoi,¹⁸ M.D. Shapiro,²⁸ T. Shears,²⁹ P.F. Shepard,⁴⁵ D. Sherman,²¹ M. Shimojima,⁵³
 M. Shochet,¹³ Y. Shon,⁵⁷ I. Shreyber,³⁵ A. Sidoti,⁴⁴ A. Sill,¹⁶ P. Sinervo,³² A. Sisakyan,¹⁴
 J. Sjolín,⁴¹ A. Skiba,²⁵ A.J. Slaughter,¹⁶ K. Sliwa,⁵⁴ D. Smirnov,³⁶ J. R. Smith,⁷
 F.D. Snider,¹⁶ R. Snihur,³² M. Soderberg,³³ A. Soha,⁷ S. Somalwar,⁵⁰ V. Sorin,³⁴
 J. Spalding,¹⁶ F. Spinella,⁴⁴ P. Squillacioti,⁴⁴ M. Stanitzki,⁵⁸ A. Staveris-Polykalas,⁴⁴

R. St. Denis,²⁰ B. Stelzer,⁸ O. Stelzer-Chilton,³² D. Stentz,³⁷ J. Strologas,³⁶ D. Stuart,¹⁰
 J.S. Suh,²⁷ A. Sukhanov,¹⁷ K. Sumorok,³¹ H. Sun,⁵⁴ T. Suzuki,⁵³ A. Taffard,²³
 R. Tafirout,³² R. Takashima,³⁹ Y. Takeuchi,⁵³ K. Takikawa,⁵³ M. Tanaka,² R. Tanaka,³⁹
 M. Tecchio,³³ P.K. Teng,¹ K. Terashi,⁴⁸ S. Tether,³¹ J. Thom,¹⁶ A.S. Thompson,²⁰
 E. Thomson,⁴³ P. Tipton,⁴⁷ V. Tiwari,¹² S. Tkaczyk,¹⁶ D. Toback,⁵¹ K. Tollefson,³⁴
 T. Tomura,⁵³ D. Tonelli,⁴⁴ M. Tönnemann,³⁴ S. Torre,⁴⁴ D. Torretta,¹⁶ S. Tourneur,¹⁶
 W. Trischuk,³² R. Tsuchiya,⁵⁵ S. Tsuno,³⁹ N. Turini,⁴⁴ F. Ukegawa,⁵³ T. Unverhau,²⁰
 S. Uozumi,⁵³ D. Usynin,⁴³ L. Vacavant,²⁸ A. Vaiciulis,⁴⁷ S. Vallecorsa,¹⁹ A. Varganov,³³
 E. Vataga,³⁶ G. Velez,¹⁶ G. Veramendi,²³ V. Veszpremi,⁴⁶ T. Vickey,²³ R. Vidal,¹⁶ I. Vila,¹¹
 R. Vilar,¹¹ I. Vollrath,³² I. Volobouev,²⁸ F. Würthwein,⁹ P. Wagner,⁵¹ R. G. Wagner,²
 R.L. Wagner,¹⁶ W. Wagner,²⁵ R. Wallny,⁸ T. Walter,²⁵ Z. Wan,⁵⁰ M.J. Wang,¹
 S.M. Wang,¹⁷ A. Warburton,³² B. Ward,²⁰ S. Waschke,²⁰ D. Waters,³⁰ T. Watts,⁵⁰
 M. Weber,²⁸ W.C. Wester III,¹⁶ B. Whitehouse,⁵⁴ D. Whiteson,⁴³ A.B. Wicklund,²
 E. Wicklund,¹⁶ H.H. Williams,⁴³ P. Wilson,¹⁶ B.L. Winer,³⁸ P. Wittich,⁴³ S. Wolbers,¹⁶
 C. Wolfe,¹³ S. Worm,⁵⁰ T. Wright,³³ X. Wu,¹⁹ S.M. Wynne,²⁹ S. Xie,³² A. Yagil,¹⁶
 K. Yamamoto,⁴⁰ J. Yamaoka,⁵⁰ Y. Yamashita,³⁹ C. Yang,⁵⁸ U.K. Yang,¹³ W.M. Yao,²⁸
 G.P. Yeh,¹⁶ J. Yoh,¹⁶ K. Yorita,¹³ T. Yoshida,⁴⁰ I. Yu,²⁷ S.S. Yu,⁴³ J.C. Yun,¹⁶
 L. Zanello,⁴⁹ A. Zanetti,⁵² I. Zaw,²¹ F. Zetti,⁴⁴ X. Zhang,²³ J. Zhou,⁵⁰ and S. Zucchelli⁵

(CDF Collaboration)

¹*Institute of Physics, Academia Sinica,*

Taipei, Taiwan 11529, Republic of China

²*Argonne National Laboratory, Argonne, Illinois 60439*

³*Institut de Fisica d'Altes Energies,*

Universitat Autònoma de Barcelona,

E-08193, Bellaterra (Barcelona), Spain

⁴*Baylor University, Waco, Texas 76798*

⁵*Istituto Nazionale di Fisica Nucleare,*

University of Bologna, I-40127 Bologna, Italy

⁶*Brandeis University, Waltham, Massachusetts 02254*

⁷*University of California, Davis, Davis, California 95616*

- ⁸*University of California, Los Angeles, Los Angeles, California 90024*
- ⁹*University of California, San Diego, La Jolla, California 92093*
- ¹⁰*University of California, Santa Barbara, Santa Barbara, California 93106*
- ¹¹*Instituto de Fisica de Cantabria, CSIC-University of Cantabria, 39005 Santander, Spain*
- ¹²*Carnegie Mellon University, Pittsburgh, PA 15213*
- ¹³*Enrico Fermi Institute, University of Chicago, Chicago, Illinois 60637*
- ¹⁴*Joint Institute for Nuclear Research, RU-141980 Dubna, Russia*
- ¹⁵*Duke University, Durham, North Carolina 27708*
- ¹⁶*Fermi National Accelerator Laboratory, Batavia, Illinois 60510*
- ¹⁷*University of Florida, Gainesville, Florida 32611*
- ¹⁸*Laboratori Nazionali di Frascati, Istituto Nazionale
di Fisica Nucleare, I-00044 Frascati, Italy*
- ¹⁹*University of Geneva, CH-1211 Geneva 4, Switzerland*
- ²⁰*Glasgow University, Glasgow G12 8QQ, United Kingdom*
- ²¹*Harvard University, Cambridge, Massachusetts 02138*
- ²²*Division of High Energy Physics, Department of Physics,
University of Helsinki and Helsinki Institute of Physics, FIN-00014, Helsinki, Finland*
- ²³*University of Illinois, Urbana, Illinois 61801*
- ²⁴*The Johns Hopkins University, Baltimore, Maryland 21218*
- ²⁵*Institut für Experimentelle Kernphysik,
Universität Karlsruhe, 76128 Karlsruhe, Germany*
- ²⁶*High Energy Accelerator Research Organization (KEK), Tsukuba, Ibaraki 305, Japan*
- ²⁷*Center for High Energy Physics: Kyungpook National University,
Taegu 702-701; Seoul National University,
Seoul 151-742; and SungKyunKwan University, Suwon 440-746; Korea*
- ²⁸*Ernest Orlando Lawrence Berkeley National Laboratory, Berkeley, California 94720*
- ²⁹*University of Liverpool, Liverpool L69 7ZE, United Kingdom*
- ³⁰*University College London, London WC1E 6BT, United Kingdom*
- ³¹*Massachusetts Institute of Technology, Cambridge, Massachusetts 02139*
- ³²*Institute of Particle Physics: McGill University, Montréal,
Canada H3A 2T8; and University of Toronto, Toronto, Canada M5S 1A7*
- ³³*University of Michigan, Ann Arbor, Michigan 48109*

- ³⁴*Michigan State University, East Lansing, Michigan 48824*
- ³⁵*Institution for Theoretical and Experimental Physics, ITEP, Moscow 117259, Russia*
- ³⁶*University of New Mexico, Albuquerque, New Mexico 87131*
- ³⁷*Northwestern University, Evanston, Illinois 60208*
- ³⁸*The Ohio State University, Columbus, Ohio 43210*
- ³⁹*Okayama University, Okayama 700-8530, Japan*
- ⁴⁰*Osaka City University, Osaka 588, Japan*
- ⁴¹*University of Oxford, Oxford OX1 3RH, United Kingdom*
- ⁴²*University of Padova, Istituto Nazionale di Fisica Nucleare,
Sezione di Padova-Trento, I-35131 Padova, Italy*
- ⁴³*University of Pennsylvania, Philadelphia, Pennsylvania 19104*
- ⁴⁴*Istituto Nazionale di Fisica Nucleare Pisa, Universities of Pisa,
Siena and Scuola Normale Superiore, I-56127 Pisa, Italy*
- ⁴⁵*University of Pittsburgh, Pittsburgh, Pennsylvania 15260*
- ⁴⁶*Purdue University, West Lafayette, Indiana 47907*
- ⁴⁷*University of Rochester, Rochester, New York 14627*
- ⁴⁸*The Rockefeller University, New York, New York 10021*
- ⁴⁹*Istituto Nazionale di Fisica Nucleare, Sezione di Roma 1,
University of Rome “La Sapienza,” I-00185 Roma, Italy*
- ⁵⁰*Rutgers University, Piscataway, New Jersey 08855*
- ⁵¹*Texas A&M University, College Station, Texas 77843*
- ⁵²*Istituto Nazionale di Fisica Nucleare, University of Trieste/ Udine, Italy*
- ⁵³*University of Tsukuba, Tsukuba, Ibaraki 305, Japan*
- ⁵⁴*Tufts University, Medford, Massachusetts 02155*
- ⁵⁵*Waseda University, Tokyo 169, Japan*
- ⁵⁶*Wayne State University, Detroit, Michigan 48201*
- ⁵⁷*University of Wisconsin, Madison, Wisconsin 53706*
- ⁵⁸*Yale University, New Haven, Connecticut 06520*

(Dated: September 1, 2005)

Abstract

We report two measurements of the top quark mass M_{top} using the CDF II detector at the Fermilab Tevatron in a 318 pb^{-1} data sample observed in the lepton + jets final state. One method uses an event-based likelihood technique resulting in $M_{\text{top}} = 173.2^{+2.6}_{-2.4} \text{ (stat.)} \pm 3.2 \text{ (syst.) GeV}/c^2$ or $173.2^{+4.1}_{-4.0} \text{ GeV}/c^2$. The second method reconstructs a top quark mass in each event using the measured invariant mass of the hadronically decaying W boson to constrain the jet energy scale to obtain a value for M_{top} of $173.5^{+3.7}_{-3.6} \text{ (stat.)} \pm 1.3 \text{ (syst.) GeV}/c^2$ or $173.5^{+3.9}_{-3.8} \text{ GeV}/c^2$. The latter is the most precise single measurement of this important physical parameter.

PACS numbers: 14.65.Ha, 12.15.Ff

The top quark is the heaviest known elementary particle with a mass 40 times that of the next-heaviest quark or lepton. Because of this comparatively large mass, top quark studies provide insight into our understanding of mass in general, and test theories that explain the large range of quark and lepton masses. Within the context of the Standard Model of particle physics, the top quark mass is related to the masses of the W boson and the Higgs boson, the latter object being the key to our understanding of the origin of mass [1]. Precision measurements of the top quark and W boson masses test the consistency of the Standard Model, and in particular the Higgs mechanism. An improved measurement of the top quark mass is therefore a main goal of the experiments at the Fermilab Tevatron collider.

In this Letter we present two measurements of the top quark mass in the lepton + jets decay channel. We use a sample of $t\bar{t}$ decays corresponding to 318 pb^{-1} of proton-antiproton collisions at $\sqrt{s} = 1.96 \text{ TeV}$ and collected using the Collider Detector at Fermilab (CDF II) between February 2002 and August 2004. In the lepton + jets channel, $t\bar{t}$ pair production is followed by the decay of each top quark to a W boson and a b quark, the hadronic decay of one W boson, and the leptonic decay of the other. This decay channel has the largest branching fraction with good signal-to-background, allowing accurate top quark mass measurements. Events in this channel contain an electron or muon and a neutrino from the leptonic W boson decay, two quark jets from the hadronic W boson decay, and two b -quark jets.

We select events consistent with this decay topology and analyze them using two complementary methods. Both methods have a top quark mass accuracy 30% greater than earlier results, and have different statistical and systematic uncertainties. The first method uses an event-by-event likelihood analysis employing the full matrix element for $t\bar{t}$ production and decay to extract a joint likelihood as a function of the top quark mass, M_{top} . This technique, known as the “dynamical likelihood method” or DLM, was developed by the CDF collaboration [2] and is similar to that used by the DØ collaboration to make the previous most precise measurement of the top quark mass [3]. A second method, developed by the CDF collaboration [4], reconstructs a top quark mass, m_t^{reco} , in each event and compares the distribution of m_t^{reco} with template distributions derived from model calculations to estimate M_{top} . We have improved this “template method” by using the fact that the hadronically decaying W boson daughters should form a final state whose invariant mass is consistent with the known W boson mass. This allows us to constraint the dominant systematic uncertainty in earlier measurements, the jet energy scale.

The CDF II detector [5] is a general-purpose charged and neutral particle detector located at an interaction point along the Tevatron collider. The detector comprises a solenoidal charged particle spectrometer, consisting of an eight-layer silicon microstrip detector array and a cylindrical drift chamber immersed in a 1.4 T magnetic field, a segmented sampling calorimeter with acceptance up to pseudorapidity $|\eta| = 3.6$, and a set of charged particle detectors outside the calorimeter used to identify muon candidates.

Events for this analysis were selected by the presence of an electron or muon candidate with transverse momentum $p_T > 20$ GeV/ c and $|\eta| < 1$ and missing transverse energy exceeding 20 GeV, corresponding to a high-energy neutrino candidate. The signal-to-background was improved by requiring in each event the presence of four or more jets with $|\eta| < 2.0$. To reduce backgrounds further we required either (a) at least four jets with transverse energy $E_T > 21$ GeV or (b) at least three jets with $E_T > 15$ GeV and a fourth jet with $E_T > 8$ GeV with at least one jet identified as a b quark candidate through the presence of a displaced vertex within the jet arising from the decay of the long-lived bottom quark (b tag). This selection resulted in 165 events that, based on our background estimates, are primarily $t\bar{t}$ events. The methods used to estimate the backgrounds are detailed in [6].

The DLM analysis uses a subset of those data and selects events containing only four jets with $E_T > 15$ GeV where at least one of the jets has a b tag. This results in 63 events. We have estimated the various sources of background contamination in this sample, summarized in Table I, to be 9.2 ± 1.8 events. The template method subdivides the 165 events into four non-overlapping subsamples with different expected m_t^{reco} distributions and background levels. Ordered by decreasing statistical power, the subsamples are 1) events with at least four jets with $E_T > 15$ GeV and one b -tagged jet (“1-tag Tight” sample with 63 events), 2) events with two b -tagged jets (“2-tag” sample with 25 events), 3) events with a fourth jet with $8 \text{ GeV} < E_T < 15 \text{ GeV}$ and one b -tagged jet (“1-tag Loose” sample with 33 events), and 4) events with four jets with $E_T > 21$ GeV and no b -tagged jets (“0-tag” sample with 44 events). The estimated background levels in the samples with a b tag are summarized in Table I. The background level in the 0-tag sample is determined in the subsequent fit.

Both analyses use calibrated jet energies, based on a combination of instrumental calibration and analysis of data control samples [7]. The uncertainty on the jet energy scale σ_c is the major source of systematic uncertainty on M_{top} . For jets in the $t\bar{t}$ sample, σ_c is roughly

TABLE I: The background composition and the number of $t\bar{t}$ candidates for events with ≥ 1 b tag, and for the subset of them used in the DLM analysis.

	≥ 1 b tag	DLM sample
Source	Expected Background	
W + jets	19.6 ± 2.4	5.3 ± 1.1
QCD	4.7 ± 0.7	3.1 ± 1.0
Other	2.3 ± 0.2	0.8 ± 0.1
Total	26.6 ± 3.0	9.2 ± 1.8
	Identified $t\bar{t}$ Candidates	
Data	121	63

3% of the measured jet energy, depending on the η and p_T of the jet. The parameter JES is defined as the difference between our measured jet energy after calibration and the true jet energy averaged over all jets in the sample, in units of σ_c .

The DLM technique, described in detail in [8], defines a likelihood for each event based on the differential cross section per unit phase space volume of the final state partons, $d\sigma_{t\bar{t}}/d\Phi$, as a function of M_{top} . Detector resolution effects are accounted for using $t\bar{t}$ events generated by the HERWIG Monte Carlo program [9] and full detector simulation to derive transfer functions (TF). The TF relates the transverse energies of the quarks, denoted by \mathbf{x} , and the observed jets. The parton kinematics of the $t\bar{t}$ final state are constructed in the following way: We first generate a random value for the virtual mass squared of the W boson in the leptonic channel, s_W , according to the Breit-Wigner form. We identify the momentum of the electron or muon daughter with the measured value, and the neutrino transverse momentum with the measured missing transverse energy. We then generate random values for the momenta of final state quarks according to the TF probabilities. We determine the z component of the neutrino momentum, with a two-fold ambiguity, using s_W as a constraint. Thus, for a given set of \mathbf{x} and s_W , we fully determine the event kinematics, and the event likelihood as a function of M_{top} is given by

$$\mathbf{L}(M_{\text{top}}) = N \sum_{I_j} \sum_{I_\nu} \frac{d\sigma_{t\bar{t}}}{d\Phi}(M_{\text{top}}; \mathbf{x}, s_W), \quad (1)$$

where the normalization factor, N , is independent of M_{top} for a given event, and the indices

I_j and I_ν run over the parton-jet assignments and the two neutrino solutions, respectively. The event likelihood is obtained by numerically integrating over \mathbf{x} given by the TF and s_W given by the Breit-Wigner distribution.

Figure 1 shows the distribution of the top quark mass value at the point of maximum likelihood in each event compared with the expectation from simulated events. An inset shows the joint log-likelihood as a function of M_{top} , formed by multiplying the likelihoods of the individual events together. We account for the presence of background events by evaluating the small shift of $+1.4 \text{ GeV}/c^2$ they make in the measured top quark mass. From the joint likelihood we infer $M_{\text{top}} = 173.2^{+2.6}_{-2.4} \text{ (stat.) GeV}/c^2$, where the uncertainty is only statistical. The systematic uncertainty due to the jet energy scale is estimated as the shift in M_{top} arising from a $1 \sigma_c$ change in JES, and is $3.0 \text{ GeV}/c^2$.

The template method is described in detail in [10]. We perform a χ^2 minimization to fit the parton momenta from the $t\bar{t}$ daughters and determine m_t^{reco} for each event, assuming that the final state arises from the decay of a $t\bar{t}$ pair into W bosons and b quarks. We use only the four leading jets in the mass reconstruction. In the χ^2 fit, both sets of W decay daughters are constrained to have the invariant mass of the W boson, and both Wb states are constrained to have the same mass. The ambiguity arising from the different ways of assigning the jets to the four quarks is resolved by selecting the assignment with the lowest χ^2 , taking into account the b -tagging information. We construct a histogram of m_t^{reco} for each subsample, discarding events with $\chi^2 > 9$, corresponding to poorly reconstructed or background events.

The parameter JES is determined within this event sample by removing the W boson mass constraints, and identifying for each event all pairs of jets that would be consistent with the W boson final state. We form histograms of the invariant masses of these jet pairs for each of the four event subsamples and compare these with what we expect given the precisely known W boson mass [11].

We use these eight histograms to measure simultaneously M_{top} and JES. An unbinned likelihood fit is performed to parameterized signal templates taken from simulated $t\bar{t}$ events generated using different values of M_{top} and JES, and background templates derived from studies of the relevant background processes. We include in the fit a Gaussian constraint ($\text{JES} = 0 \pm 1 \sigma_c$) from the extrinsic jet energy calibrations, and we constrain the background rates in the 2-tag, 1-tag Tight, and 1-tag Loose samples to the estimated background

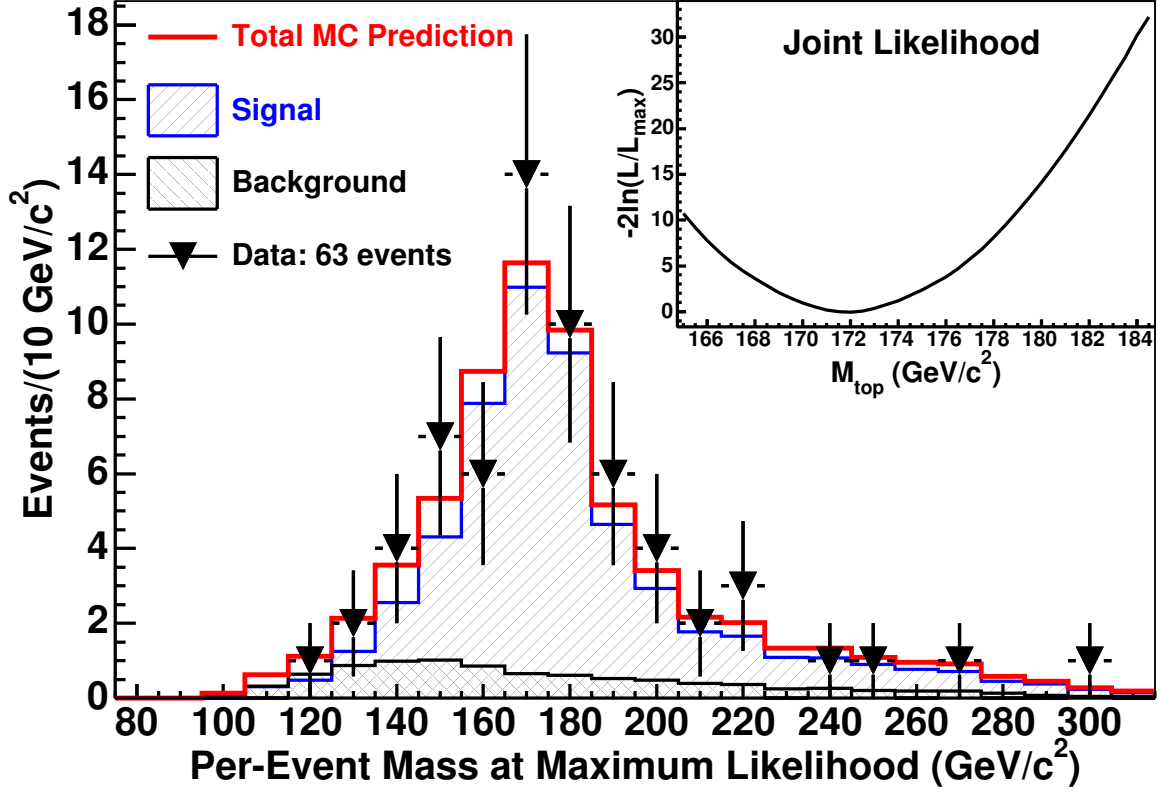


FIG. 1: The value of the top quark mass at the maximum of the DLM likelihood is plotted for each event. Data events (points) are compared to an expected distribution (histogram) comprising simulated $t\bar{t}$ ($M_{\text{top}} = 172.5 \text{ GeV}/c^2$) and background events. The last point is an overflow bin. The inset shows the joint log likelihood for the 63 events, before accounting for the presence of background.

rates within their uncertainties. The background level in the 0-tag sample is determined in the fit using the differences in predicted signal and background mass distributions to be $15.7^{+8.0}_{-7.1} \text{ (stat.) events}$.

The four reconstructed top quark mass distributions and the results of the fit are shown in Fig. 2, where we also show the background contributions. In all cases, we see agreement between the observed data distributions and the fitted curves. We obtain $M_{\text{top}} = 173.5^{+3.7}_{-3.6} \text{ (stat.) GeV}/c^2$, where the uncertainty is statistical and incorporates the uncertainty due to JES, which we estimate contributes $\sim 2.5 \text{ GeV}/c^2$. Figure 3 shows the likelihood in the M_{top} -JES plane for the combined measurement. If we do not constrain JES to the nominal value of zero, we obtain $\text{JES} = -0.25 \pm 1.22 \sigma_c$, which indicates our

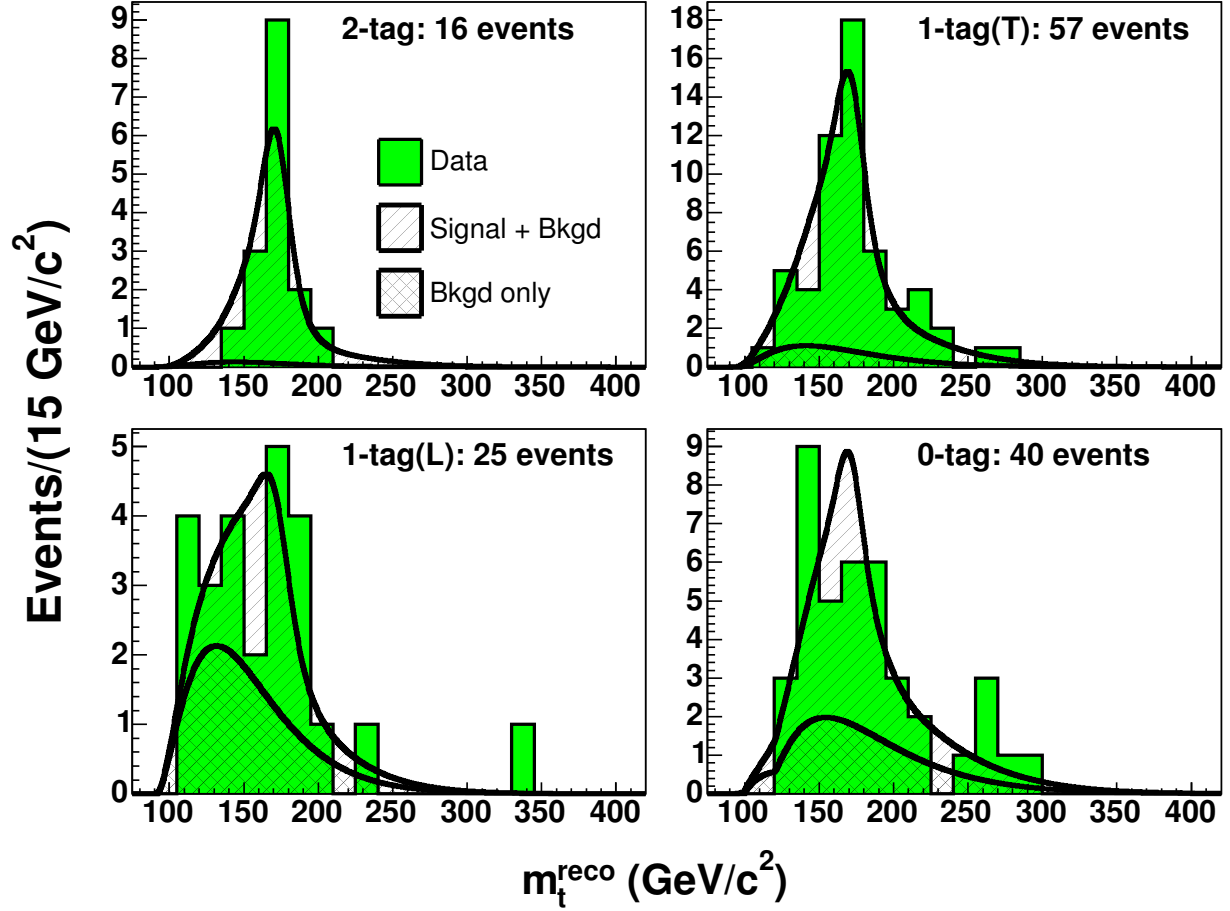


FIG. 2: The m_t^{reco} distribution of the template method is shown for each subsample overlaid with the expected distribution using the top quark mass, jet energy scale, and signal and background normalizations from the combined fit.

nominal jet energy calibrations are in good agreement with information provided by the W boson mass peak in the $t\bar{t}$ decay. This also demonstrates that the JES constraint from the W boson decay has comparable precision to the jet energy calibration.

There are a number of additional systematic uncertainties that affect both analyses: initial state and final state radiation uncertainties (ISR/FSR); uncertainties arising from the parton distribution functions (PDFs); and uncertainties arising from b -jet fragmentation, decays, and color connections, modeling of the background processes, and the event generators we employ (Modeling). Table II summarizes these uncertainties.

The DLM method has additional uncertainties that arise from the use of transfer functions and from the procedure that corrects the measured mass for the presence of background (Method). Together with the JES and other common sources noted above, the systematic

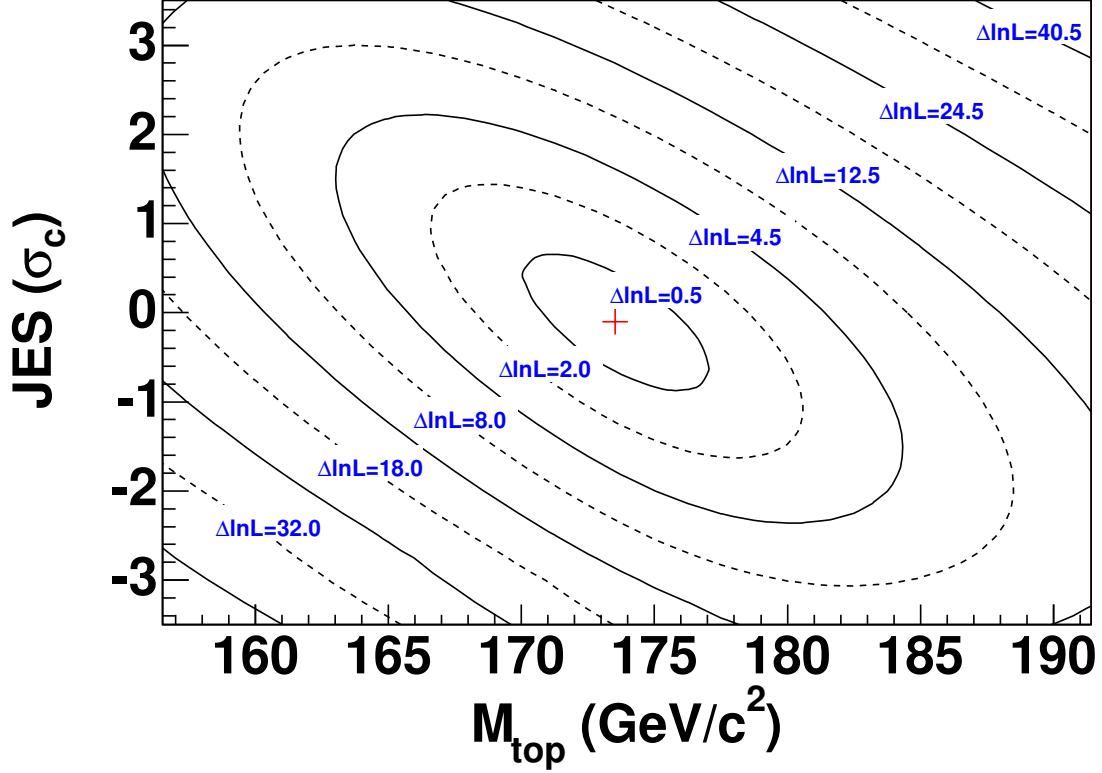


FIG. 3: Contours of the template method likelihood are shown in the M_{top} -JES plane for the combined fit to all four subsamples. The crosshair shows the best fit point. Contours are given at intervals of $\Delta \ln L$, the change in log-likelihood from its maximum.

TABLE II: The systematic uncertainties for the two analyses.

Systematic	DLM	Template
	ΔM_{top} (GeV/ c^2)	ΔM_{top} (GeV/ c^2)
Jet Energy Scale	3.0	$[\sim 2.5]^a$
ISR/FSR	0.6	0.7
PDFs	0.5	0.3
Modeling	0.8	0.9
Method	0.5	0.6
Total	3.2	1.3^a

^aThe JES systematic is included in the uncertainty reported by the likelihood fit.

uncertainty on the DLM mass measurement is $3.2 \text{ GeV}/c^2$. The template method has additional uncertainties arising from the statistical precision of the templates themselves and approximations made in treating JES as a single parameter affecting all jets coherently (Method). Excluding JES, the total systematic uncertainty on the template mass measurement is $1.3 \text{ GeV}/c^2$.

In summary, we have presented two new measurements of the top quark mass. An analysis using the DLM method results in $M_{\text{top}} = 173.2^{+2.6}_{-2.4} \text{ (stat.)} \pm 3.2 \text{ (syst.) GeV}/c^2$; the analysis using the template technique results in $M_{\text{top}} = 173.5^{+3.7}_{-3.6} \text{ (stat.)} \pm 1.3 \text{ (syst.) GeV}/c^2$. There is a large statistical correlation between these measurements given the common data sample so that we quote as a result only the more accurate measurement, the template method result of $M_{\text{top}} = 173.5^{+3.9}_{-3.8} \text{ GeV}/c^2$. This provides the most precise single constraint on this important physical parameter, exceeding the accuracy of the previous world average for the top quark mass [11].

We thank the Fermilab staff and the technical staffs of the participating institutions for their vital contributions. This work was supported by the U.S. Department of Energy and National Science Foundation; the Italian Istituto Nazionale di Fisica Nucleare; the Ministry of Education, Culture, Sports, Science and Technology of Japan; the Natural Sciences and Engineering Research Council of Canada; the National Science Council of the Republic of China; the Swiss National Science Foundation; the A.P. Sloan Foundation; the Bundesministerium für Bildung und Forschung, Germany; the Korean Science and Engineering Foundation and the Korean Research Foundation; the Particle Physics and Astronomy Research Council and the Royal Society, UK; the Russian Foundation for Basic Research; the Comisión Interministerial de Ciencia y Tecnología, Spain; in part by the European Community's Human Potential Programme under contract HPRN-CT-2002-00292; and the Academy of Finland.

-
- [1] J. Erler and P. Langacker, Phys. Lett. **B592**, 1 (2004).
 - [2] K. Kondo, J. Phys. Soc. Jap. **57**, 4126 (1988).
 - [3] V. M. Abazov *et al.* (D0 Collaboration), Nature **429**, 638 (2004).
 - [4] F. Abe *et al.* (CDF Collaboration), Phys. Rev. **D50**, 2966 (1994).

- [5] D. Acosta *et al.* (CDF Collaboration), Phys. Rev. **D71**, 032001 (2005), we employ a cylindrical coordinate system where θ and ϕ are the polar and azimuthal angle, respectively, with respect to the proton beam. Pseudorapidity is $\eta = -\ln \tan(\theta/2)$. Transverse energy and momentum are $E_T = E \sin \theta$ and $p_T = p \sin \theta$, respectively, where E and p are energy and momentum. Missing transverse energy is $|\sum_i E_T^i \mathbf{n}_i|$, where \mathbf{n}_i is the unit vector in the transverse plane pointing from the beamline to the i th calorimeter tower.
- [6] D. Acosta *et al.* (CDF Collaboration), Phys. Rev. **D71**, 052003 (2005).
- [7] B. B. *et al.*, to be submitted to Nucl. Instrum. Methods A.
- [8] A. Abulencia *et al.* (CDF Collaboration), to be submitted to Phys. Rev. D.
- [9] G. Corcella, I. G. Knowles, G. Marchesini, S. Moretti, K. Odagiri, P. Richardson, M. H. Seymour, and B. R. Webber, JHEP **01**, 010 (2001), [hep-ph/0011363]; hep-ph/0210213.
- [10] A. Abulencia *et al.* (CDF Collaboration), to be submitted to Phys. Rev. D.
- [11] S. Eidelman *et al.* (Particle Data Group Collaboration), Phys. Lett. **B592**, 1 (2004).